Bacterial Expression and Characterization of a Novel, Soluble, Calcium-Binding, and Calcium-Activated Human Nucleotidase†

Deirdre M. Murphy, Vasily V. Ivanenkov, and Terence L. Kirley*

Department of Pharmacology and Cell Biophysics, College of Medicine, University of Cincinnati, P.O. Box 670575, Cincinnati, Ohio 45267-0575

Received August 29, 2002; Revised Manuscript Received November 20, 2002

ABSTRACT: A newly discovered human analogue of a bed bug apyrase, which we named hSCAN-1 for human soluble calcium-activated nucleotidase-1, was expressed in bacteria, refolded from inclusion bodies, purified, and characterized. This apyrase, which is distinct from the eNTPDases exemplified by the endothelial CD39 (NTPDase1) apyrase, is a 38 kDa monomeric enzyme capable of hydrolyzing a variety of nucleoside di- and triphosphates, but not monophosphates. Preferred substrates include GDP, UDP, and IDP, with a pH optimum for activity between 6 and 7. The specific activity and substrate preference of the bacterially expressed enzyme closely mimic those of the enzyme expressed in mammalian COS cells, as well as the enzyme synthesized in an in vitro bacterial expression system. This suggests that glycosylation and other posttranslational modifications that do not occur in bacteria are not necessary for nucleotidase activity or proper folding of this human apyrase. hSCAN-1 absolutely requires Ca^{2+}, but not Mg^{2+} or other divalent cations analyzed, for enzymatic activity. Surprisingly, the activity does not increase in a quasi-linear fashion at sub-millimolar Ca^{2+} concentrations, as would be expected if Ca^{2+} were only used as a cosubstrate for the nucleotide substrate, but rather follows a sigmoidal curve. The intrinsic fluorescence and difference absorption studies of hSCAN-1 in the absence of nucleotides revealed Ca^{2+}-induced changes in the environment of tryptophan and tyrosine residues with half-saturation at about 90 μM Ca^{2+}. NaCl increased the half-saturating Ca^{2+} concentration needed for both structural changes detected by optical spectroscopy and enzymatic activation of hSCAN-1 detected by nucleotidase assay. These results suggest that Ca^{2+} triggers a conformational change in hSCAN-1, converting the enzymatically inactive protein to the active enzyme, in addition to forming the metal−nucleotide substrate complex necessary for nucleotidase activity.

Apyrases are enzymes that hydrolyze nucleoside di- and triphosphates. The eNTPDases[1] represent one such family of apyrases. This family consists of at least six members; NTPDase1−4 are membrane bound, while NTPDase5,6 are released as soluble enzymes (*1*). Very recently, a human homologue of the blood-sucking insect soluble apyrases, exemplified by the *Cimex* bed bug apyrase (*2*), was cloned, sequenced, and expressed in mammalian cells (*3*). We have named this apyrase hSCAN-1, for human soluble calcium-activated nucleotidase-1. The distribution of this human homologue of the bed bug apyrase was determined by Smith et al., and the highest levels of mRNA were found in testes, prostate, placenta, and small intestine (*3*). Such a soluble mammalian nucleotidase has the potential for therapeutic use for modulation of processes controlled by P_2 purinergic receptors, acting via hydrolysis of the nucleotide agonists of these receptors. In addition, these enzymes convert the nucleoside di-and triphosphates into nucleoside monophosphates and nucleosides, in conjunction with 5′-ectonucleotidases. Thus, hydrolysis of these nucleotides by apyrases not only depletes the di- or triphosphate agonists at a given P_2 receptor, but also generates agonists for P_1 receptors which, when activated, often mediate different, and sometimes opposite, physiological effects. Therefore, the discovery, characterization, and large-scale synthesis of soluble human apyrases are important for understanding and manipulating these systems. The modulation of physiological processes controlled by purinergic receptor systems, including platelet aggregation and blood clotting mediated by ADP (*4*), smooth muscle contraction mediated by ATP purinergic signaling (*5*), and nociception, where ATP is recognized to play an important role in pain perception mediated by P_{2X} receptors (*6*, *7*), is an attractive potential therapeutic target for the introduction of, and the inhibition of, soluble human apyrase enzymes.

In this work, we describe the first bacterial expression of a human apyrase, as well as conditions needed to refold the insoluble protein from inclusion bodies into an active conformation. Enzymatic characterization of the expressed enzyme demonstrates that it does not hydrolyze nucleoside monophosphates and, unlike the eNTPDase apyrases, can only utilize calcium, but not magnesium, as the divalent cation required for the hydrolysis of nucleoside di- and

† This work was supported by NIH Grant HL59915.

* To whom correspondence should be addressed. Phone: (513) 558-2353. Fax: (513) 558-1169. E-mail: terry.kirley@uc.edu.

[1] Abbreviations: hSCAN-1, human soluble calcium-activated nucleotidase-1 (GenBank accession number AF328554); eNTPDase, ectonucleoside triphosphate diphosphohydrolase; CD, circular dichroism; MOPS, 3-(*N*-morpholino)propanesulfonic acid; P_i, inorganic phosphate; IPTG, isopropyl-β-D-thiogalactopyranoside; B-PER, bacterial protein extraction reagent; Ca−ADP, calcium−ADP complex; Ca−GDP, calcium−GDP complex.

10.1021/bi026763b CCC: $25.00
Published on Web 02/01/2003

triphosphates. It was previously demonstrated that mammalian COS cell expressed hSCAN-1 also requires Ca^{2+} for nucleotidase activity (*3*). That recent study also showed that the mammalian cell expressed enzyme preferentially hydrolyzes UDP and GDP, with slower hydrolysis of UTP, GTP, ADP, and ATP, with a pH optimum of the enzyme in the range of 6.2−7.2 (*3*). Thus, the bacterially expressed and refolded enzyme described in this study has properties very similar to the enzyme expressed in mammalian COS cells, indicating that posttranslational modifications such as glycosylation that do not occur in bacteria are not necessary for the synthesis of active and properly folded hSCAN-1 apyrase.

In the present study, we demonstrate that this soluble human apyrase is a calcium-binding protein, as evident from saturable Ca^{2+}-dependent changes in the intrinsic tryptophan fluorescence, UV difference absorption spectra, and Ca^{2+}-triggered transition from the enzymatically inactive form to the active enzyme. The large-scale bacterial expression and refolding scheme described in this work will facilitate future crystallization and X-ray structural determination of this human apyrase.

MATERIALS AND METHODS

Materials. The QuickChange site-directed mutagenesis kit and *Escherichia coli* XL-1 Blue competent cells were purchased from Stratagene. The DNA Core Facility at the University of Cincinnati produced the synthetic oligonucleotides and performed DNA sequencing. Plasmid purification kits and Ni−NTA agarose were purchased from Qiagen Inc. *Nhe*I and *Not*I restriction endonucleases, T4 DNA ligase, and the mammalian expression vector pcDNA3 were obtained from Invitrogen. The bacterial expression vector pET28a and the expression host *E. coli* BL21 were purchased from Novagen. Glycerol and dialysis tubing were from Fisher. B-PER bacterial extraction reagent and enhanced chemiluminescent reagents were purchased from Pierce. The rapid translation system (RTS) 100 *E. coli* HY kit was obtained from Roche Diagnostics. The 4−15% Tris−glycine gels were from Bio-Rad, and the 4−20% Express Tris−glycine gels were purchased from ISC BioExpress. Potato apyrase, kanamycin, nucleotides, IPTG, glucose, DTT, Chelex 100 resin, and other reagents were from Sigma.

Protein Assay. Protein concentrations were determined using the Bio-Rad Coomassie Brilliant Blue G-250 dye binding technique according to the modifications of Stoscheck (*8*) using bovine serum albumin as a standard.

Polyclonal Antibody Production. The production of the polyclonal antiserum to the hSCAN-1 carboxy-terminal amino acid sequence and the affinity purification of antibodies from that antiserum have been described (*3*).

Electrophoresis and Western Blot Analysis. SDS−PAGE was performed following the method of Laemmli (*9*), using 4−20% or 4−15% precast gradient gels. The hSCAN-1 samples were boiled for 5 min in SDS sample buffer containing 30 mM dithiothreitol prior to SDS−PAGE. For native gel electrophoresis, the Laemmli gel and buffer system was also used, without SDS in any component. The sample was diluted with 125 mM Tris−HCl, pH 6.8, buffer containing 25% glycerol and, without heating, was loaded onto an 8% polyacrylamide gel and electrophoresed until the Bromphenol Blue tracking dye reached the bottom of the gel. The gels were stained either for total protein with Coomassie Brilliant Blue or for calcium-activated ADPase activity using a modification of the Fiske and Subbarow ammonium molybdate/amidol technique (*10*) for visualization of P_i in the gel, as described previously (*11*).

Nucleotidase Assay. Nucleotidase activity was determined by measuring the amount of inorganic phosphate released from nucleotide substrates at 37 °C using a modification of the technique of Fiske and Subbarow (*10*) as previously described (*12*). Nucleotide hydrolyzing units are expressed in micromoles of P_i liberated per milligram of protein per hour. Generally, assays were conducted in 20 mM MOPS, pH 7.1, containing 5 mM $CaCl_2$ and 2.5 mM nucleotide substrate, but additional buffers and conditions were also used, as indicated.

Calculation of Free Ca^{2+}, Ca−ADP, and Ca−GDP Concentrations. Free Ca^{2+} and Ca−nucleotide complex concentrations were calculated using the WinMaxc 2.40 program (*13*; http://www.stanford.edu/~cpatton/maxc.html). This program uses critical stability constants from the most recent version of the National Institute of Standards and Technology (NIST) database, which is based on the compilation by Martell and Smith (*14*). Because the WinMaxc program does not provide K_d for the Ca−GDP complex, it was assumed that K_d for Ca−GDP is equal to K_d for Ca−ADP.

Mutagenesis of hSCAN-1 for Cloning into a Bacterial Expression Vector. The 1744 bp cDNA IMAGE clone encoding hSCAN-1 was obtained from Incyte Genomics, Inc. (GenBank EST accession number AA632390; clone ID 1131402) and cloned into pcDNA3 mammalian expression vector as described (*3*). The sequence of this cDNA has been assigned the GenBank accession number AF328554 . The putative hSCAN-1 signal peptide was identified using the computer program PSORT II, which predicted a cleavable signal peptide at residues 37 and 38 (amino acids Gly-Arg). An *Nhe*I endonuclease site was introduced by site-directed mutagenesis at the 5′-end of cDNA encoding the N-terminus of the soluble hSCAN-1 sequence following the predicted signal peptide cleavage site. The sense primer for mutagenesis was 5′-GCCCGGCCCCC*GCTAGC***CCCCCCACCCAC**-3′, with bases encoding the *Nhe*I site italic and bases corresponding to the start of the soluble hSCAN-1 protein indicated in boldface type. Using this newly introduced *Nhe*I site at the 5′-end, and the existing *Not*I site in the pcDNA3 vector multiple cloning region at the 3′-end, the cDNA sequence encoding soluble hSCAN-1 was excised from pcDNA3 vector and ligated into pET28a bacterial expression vector (cut with the same endonucleases). The resultant vector containing the hSCAN-1 insert was transformed into a nonexpression host, *E. coli* XL-1 Blue, as described by the manufacturer. The construct was verified by DNA sequencing.

Expression of hSCAN-1 in E. coli BL21 Cells. For hSCAN-1 expression, pET28a vector containing the hSCAN-1 sequence was transformed into an expression host, *E. coli* BL21. A single colony was used to inoculate 50 mL of LB broth containing 30 μg/mL kanamycin and 1% glucose (to reduce basal expression) and allowed to grow to an OD_{600} of 0.9. This 50 mL culture was then added to 500 mL of the same medium and grown at 37 °C for 2 h, reaching an OD_{600}

of 0.26. IPTG was added to 1 mM final concentration and growth of the induced culture continued for 5 h. The bacteria were harvested by centrifugation at 5000 rpm for 15 min at 4 °C and the pellets resuspended in 20 mL of the Pierce B-PER reagent. B-PER (bacterial protein extraction reagent) is a mild, nonionic, proprietary detergent in 20 mM Tris−HCl (pH 7.5) used to extract soluble proteins from inclusion bodies. The inclusion body preparation was performed as recommended by the manufacturer, resulting in 49 mg of inclusion body protein from the 550 mL bacterial culture.

Preparative Refolding of hSCAN-1 from Inclusion Bodies. A 12 mg sample of inclusion bodies was solubilized and denatured at a protein concentration of 0.6 mg/mL in 6 M Gu−HCl, 100 mM Tris−HCl, pH 8.2, containing 2 mM EDTA and 10 mM DTT for 10 min at 60 °C. After being cooled to room temperature (22 °C), the sample was diluted 10-fold with 6 M Gu−HCl, 100 mM Tris−HCl, pH 8.2, and dialyzed versus 20 volumes of 50 mM Tris−HCl, pH 8.0, 250 mM NaCl, 2 mM $CaCl_2$, and 5% glycerol for 2−3 days at 4 °C.

Purification of the Refolded hSCAN-1 Protein via the Hexahistidine Tag. After dialysis, the sample (200 mL) was clarified by centrifugation (39000*g* for 20 min at 4 °C) and added to 3 mL of Qiagen Ni−NTA agarose beads equilibrated with wash buffer (50 mM Tris−HCl, 250 mM NaCl, 2 mM $CaCl_2$, pH 8.0). After a 1 h incubation at 22 °C with end-over-end rotation, the beads were poured into a column, washed with 20 mL of wash buffer, and then washed with 30 mL of wash buffer containing 20 mM imidazole, pH 8.1. hSCAN-1 was eluted with 12 mL of wash buffer containing 150 mM imidazole, pH 8.3, and was immediately diluted with wash buffer to a total volume of 50 mL to dilute imidazole and preserve protein solubility during subsequent thrombin cleavage.

Thrombin Cleavage and Anion Exchange Chromatography of the Partially Purified hSCAN-1 Protein. The hSCAN-1 insert in pET28a bacterial expression vector, in addition to containing an amino-terminal hexa-His tag to aid protein purification, contains a thrombin site to remove the histidine tag after purification. The construct sequence in pET28a is as follows (the thrombin cleavage site is italic): MGSSH HHHHHSSG*LVPR-GS*HMAS**PPTHNAHN...EGIEFI**. The thrombin cleavage occurs between arginine and glycine residues as indicated by a hyphen, thus leaving six extra amino acid residues attached to the N-terminus of the putative, soluble hSCAN-1 sequence, which is indicated in bold. After thrombin cleavage, the purified protein (including the GSHMAS sequence at the N-terminus) is 339 amino acid residues in length. Thrombin cleavage of the Ni−NTA purified protein was accomplished by adding 8 units of thrombin (Novagen) to approximately 8 mg of protein in 50 mL. The sample was then dialyzed for 24 h at 4 °C against 2 L of 50 mM Tris−HCl, 150 mM NaCl, 2 mM $CaCl_2$, pH 8.0. To prepare the sample for anion exchange chromatography, the dialysis was continued against 2 L of 20 mM MOPS, pH 7.1, for 16 h at 4 °C. The crystal-clear sample was removed from the dialysis bag and loaded onto a 5 mL Bio-Rad Econo-Pac Q cartridge equilibrated with 20 mM MOPS, pH 7.1. The anion exchange column was washed with 10 mL of 20 mM MOPS, pH 7.1, and eluted with 50 mL of a 0−500 mM NaCl gradient in 20 mM MOPS, pH 7.1. The 2 mL fractions collected from the gradient elution, as well as the unbound and wash fractions, were all assayed for calcium-activated ADPase activity. The most active fractions were pooled.

Purification and Characterization of hSCAN-1 by Size Exclusion Chromatography. After DTT was added to a final concentration of 0.2 mM, the pooled fractions were concentrated to approximately 1 mL using an Amicon Centriprep 30 centrifugal concentration unit and applied to a 43 mL bed volume, 27 cm long Sephacryl S-200 column, equilibrated in 20 mM MOPS, 100 mM NaCl, pH 7.1. Fractions of 1.25 mL were collected and assayed for calcium-activated ADPase activity. Four fractions containing the majority of the activity were pooled and used for subsequent experiments. The column was calibrated with standard proteins, and the molecular weight of hSCAN-1 was determined.

Cell-Free in Vitro hSCAN-1 Expression. A small-scale expression of hSCAN-1 was carried out in a cell-free system using the Roche Diagnostics rapid translation system kit, according to the manufacturer's protocol. In short, 12 μL of *E. coli* lysate, 10 μL of reaction mixture, 12 μL of amino acids, 1 μL of methionine, 0.5 μg of pET28a vector containing the sequence encoding soluble hSCAN-1, and 2 μL of protease inhibitor cocktail were combined and then brought to a total reaction volume of 50 μL with reaction buffer. Expression was induced by adding IPTG to a final concentration of 0.8 mM and allowed to proceed for 5 h at 30 °C, with gentle shaking. The production of green fluorescent protein (GFP) was used as a positive control for protein expression. The calcium-activated GDPase activity of expressed hSCAN-1 was measured in 20 mM MOPS buffer, pH 7.1, containing 5 mM $CaCl_2$. Expression of hSCAN-1 was confirmed by Western blot analysis using an anti-carboxy-terminal antipeptide antibody for hSCAN-1 (*3*). To measure the specific activity of the in vitro synthesized active nucleotidase that did not require refolding, we partially purified hSCAN-1 from the reaction mixture. The reaction mixture was diluted 10-fold into 50 mM Tris−HCl, 250 mM NaCl, 2 mM $CaCl_2$, pH 8.0, and allowed to bind TALON metal affinity beads (Clontech), equilibrated in the same buffer, for 10 min at room temperature. The beads were then washed with the buffer, followed by washes with the buffer containing 10 mM imidazole, pH 8.0. The enzyme was then eluted with buffer containing 100 mM imidazole (pH 8.3) and assayed for GDPase activity, as well as run on SDS−PAGE. After Coomassie Blue staining of the gel, the amount of purified hSCAN-1 protein was quantified by comparison of the hSCAN-1 stained protein band with a calibration series of BSA protein amounts loaded on the same gel, allowing calculation of the specific activity of the in vitro expressed enzyme.

Fluorescence Spectroscopy. Fluorescence spectra were obtained on an SPF-500C SLM Instruments spectrofluorometer at room temperature with excitation and emission slit widths of 7.5 nm. The intrinsic tryptophan fluorescence of hSCAN-1 was measured by exciting the sample at 295 nm and recording the emission at 300−450 nm.

UV Spectroscopy. UV absorption and difference absorption spectra were recorded with a DU-70 Beckman spectrophotometer at room temperature. Difference spectra were taken on hSCAN-1 in 20 mM MOPS, 100 mM NaCl, pH 7.1, with a protein concentration of 0.96 mg/mL as assayed by the Coomassie Brilliant Blue binding technique, which cor-

Table 1: Purification of the Bacterially Expressed and Refolded hSCAN-1[a]

sample (step)	total vol (mL)	protein concn (mg/mL)	total protein (mg)	ADPase activity [(μmol of P/mg)/h]
refolded enzyme	200	0.06	12.0	555
clarified, refolded enzyme	200	0.0563	11.3	533
Ni−NTA agarose purified enzyme (after dilution)	50	0.164	8.2	720
thrombin-treated Ni−NTA purified enzyme	50	0.147	7.35	893
QMA ion exchange purified enzyme	10.2	0.51	5.19	1058
S-200 size exclusion chromatography purified enzyme	5.2	0.96	4.99	1127

[a] Activity was measured in 20 mM MOPS, 5 mM $CaCl_2$, pH 7.1, with 2.5 mM ADP as substrate. Approximately 50 mg of bacterial inclusion bodies was obtained from a 550 mL bacterial culture. A 12 mg sample of this inclusion body preparation was used for the refolding and purification of hSCAN-1 outlined in this table. The yield of purified hSCAN-1 protein was about 5 mg.

responded to an optical density of 2.35 at 279 nm. Both the sample and the reference cells contained 500 μL of this hSCAN-1 solution, and the difference spectra were recorded before and after stepwise addition of $CaCl_2$ to the sample cell in 2 μL aliquots. To adjust the protein concentration, the same volumes of water were added to the reference cell.

Circular Dichroism Spectroscopy. Circular dichroism (CD) spectra were acquired with a Jasco 715 spectropolarimeter. Solutions of hSCAN-1 (0.16 mg/mL = 4.24 μM) were prepared in 10 mM Tris−HCl buffer, pH 7.1, and the spectra were acquired in a cell with an optical path length of 0.1 cm. Each spectrum was the average of four spectral accumulations. Data were directly converted into mean residue molar ellipticity (mre) using Jasco J700 software and then analyzed by the DICROPROT 2000 program (*15*; http://dicroprot-pbil.ibcp.fr/), which integrates into a single package several methods designed for the estimation of protein sequence secondary structure. Within the DICROPROT computer program, the K2D program (*16*; also available directly for Web data input at http://www.embl-heidelberg.de/~andrade/k2d/) was used to determine the percent α helix, β sheet, and random coil of hSCAN-1. The K2D program uses a Kohonen neural network and the circular dichroism data from 200 to 240 nm to predict the secondary structural element composition of proteins. The PROF computer program (*17*; http://www.aber.ac.uk/~phiwww/prof/) was used to predict the amounts of secondary structure directly from the amino acid sequence of hSCAN-1, to allow comparisons between the experimentally determined and predicted secondary structural element compositions of the protein.

RESULTS

Expression, Refolding, and Purification of hSCAN-1. SDS−PAGE and Western blot results indicated that hSCAN-1 protein was expressed in bacteria in an insoluble form and found almost entirely in inclusion bodies (data not shown). Several parameters were varied to determine the optimum conditions for refolding the inclusion body protein preparation into an active nucleotidase, including the use of different denaturant/solubilizing agents and the presence or absence of DTT during the denaturation/solubilization steps. The effect of pH, the presence or absence of calcium ions, and the volume ratio of the refolding/dialysis buffer to the denatured sample were all evaluated. Protein concentration was found to be the most important variable for successful refolding of denatured, solubilized hSCAN-1 inclusion body protein. Concentrations that exceeded approximately 0.06 mg/mL resulted in precipitation of the protein during dialysis and refolding. Therefore, refolding/dialysis was performed at a solubilized inclusion body protein concentration of 0.06 mg/mL or less.

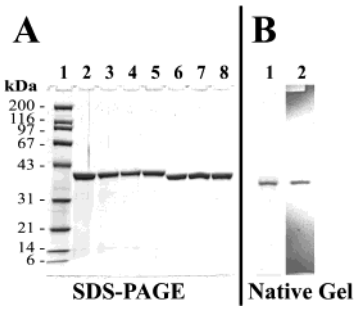

FIGURE 1: SDS−PAGE and native gel analysis of the purification and thrombin cleavage of the bacterially expressed and refolded hSCAN-1. (A) SDS−PAGE analysis of the hSCAN-1 purification steps outlined in Table 1. Bio-Rad broad range standards were loaded in lane 1, while 2 μg of protein was loaded in lanes 2−8. Lane 2: inclusion body preparation. Lane 3: refolded enzyme. Lane 4: refolded enzyme after clarification. Lane 5: Ni−NTA agarose purified enzyme. Lane 6: thrombin-treated Ni−NTA purified enzyme. Lane 7: QMA ion exchange chromatography purified enzyme. Lane 8: S-200 size exclusion chromatography purified enzyme. Note the decrease in apparent molecular weight of the protein after removal of the hexahistidine tag by thrombin cleavage (lanes 6−8). (B) Conformational homogeneity of the hSCAN-1 analyzed by native gel electrophoresis. Lane 1 contains 1 μg of hSCAN-1, stained with Coomassie Brilliant Blue for total protein. In lane 2, 1 μg of hSCAN-1 was stained for calcium-activated ADPase activity as described in the Materials and Methods. Note that the appearance of the single total protein band in lane 1 is identical with that of the nucleotidase activity band in lane 2.

The purification of the bacterially expressed and refolded hSCAN-1 and the removal of its N-terminal hexahistidine tag are summarized in Table 1. Figure 1A shows the SDS−PAGE analysis of the samples obtained after successive steps of the purification procedure listed in Table 1 and illustrates the protein homogeneity of hSCAN-1 after purification. Immobilized metal affinity chromatography resulted in a 23% increase in the ADPase specific activity of hSCAN-1. The decrease in molecular weight of hSCAN-1 after removal of the hexahistidine tag by thrombin treatment can be seen in lanes 6−8 in Figure 1A. QMA ion exchange chromatography removed thrombin, the excised hexahistidine tag, and other charged impurities. The last purification step was size exclusion chromatography, yielding purified hSCAN-1 with an ADPase activity of 1127 (μmol of P_i/mg of protein)/h. The final yield was approximately 5 mg of pure, active hSCAN-1 protein from 12 mg of insoluble, inactive inclusion body protein. The specific activity of the purified and thrombin-treated protein is only roughly doubled relative to

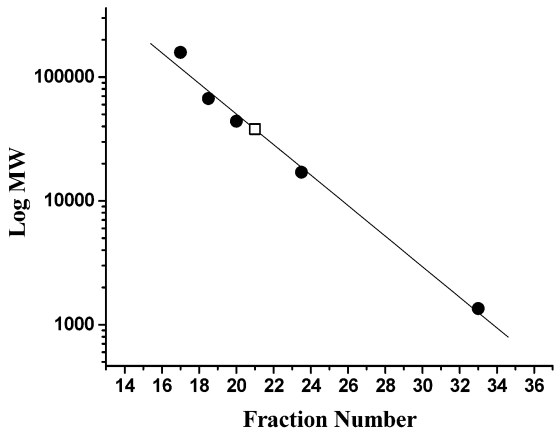

FIGURE 2: Analysis of hSCAN-1 by size exclusion chromatography on Sephacryl S-200. The calibration standards (bovine γ globulin (158 kDa), bovine serum albumin (67 kDa), ovalbumin (44 kDa), myoglobin (17 kDa), and vitamin B-12 (1.35 kDa)) are represented by filled circles, and the fraction containing the maximum calcium-activated ADPase activity is indicated by an open square. From the straight line fit of the calibration protein data, the molecular weight of the soluble hSCAN-1 was calculated to be 38 kDa.

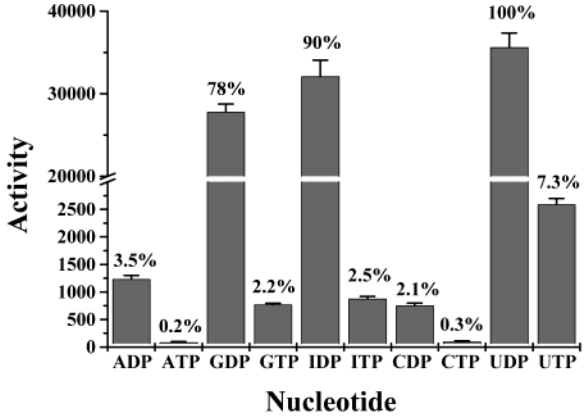

FIGURE 3: Substrate preference of hSCAN-1. Assays were done in 20 mM MOPS buffer, pH 7.1, containing 10 mM $CaCl_2$ and a final nucleotide concentration of 2.5 mM. Activity units are micromoles of P_i liberated per milligram of protein per hour at 37 °C. The break in the *y*-axis denotes a nearly 10-fold change in scale. The standard deviation of the mean for four measurements is reported. The relative activities toward various nucleotides under the conditions used are given directly above each data bar (percent maximal activities, normalized to UDPase as 100%).

that of the refolded enzyme because the inclusion body preparation was more than 50% pure hSCAN-1 protein.

The conformational homogeneity of the refolded, purified enzyme was assessed both by size exclusion chromatography (Figure 2, note that the determined molecular weight of 38000 Da is very close to that calculated from the protein sequence assuming a monomeric protein, i.e., 37770 Da), and native gel electrophoresis (Figure 1B). In Figure 1B, the native gel electrophoretic mobility of the hSCAN-1 protein band in lane 1 (stained with Coomassie) corresponds precisely to the mobility of the hSCAN-1 band stained for enzyme activity (lane 2). Electrophoretic migration of hSCAN-1 protein as a single band, as detected by both total protein (Figure 1B, lane 1) and nucleotidase activity (Figure 1B, lane 2), demonstrates the conformational homogeneity of the refolded protein.

We compared the specific activity of the enzyme refolded from bacterial inclusion bodies to that of the enzyme synthesized in active form in an in vitro system. This comparison was used as an additional indication of the efficacy and completeness of the protein refolding process. The same pET28a expression vector containing the soluble hSCAN-1 sequence that was used for bacterial expression was also used for expression with the in vitro RTS marketed by Roche. With this RTS, we obtained small amounts of active, soluble apyrase, with a specific activity of approximately 28000 (μmol of GDP hydrolyzed/mg of protein)/h (measured using 2.5 mM GDP) after purification via the hexahistidine tag. This value of specific activity of the in vitro expressed enzyme was comparable to the specific activity of hSCAN-1 that was expressed in bacteria, refolded and purified (28000−44000 (μmol/mg)/h; see Figures 3, 4, and 5).

Thus, an efficient large-scale protocol for hSCAN-1 expression, refolding, and purification was developed, and all the characterization data suggest that the bacterially expressed and refolded enzyme is in a homogeneous, enzymatically active conformation.

Biochemical Characterization of Refolded hSCAN-1. To characterize the bacterially expressed hSCAN-1 and to compare it with the same enzyme synthesized in mammalian COS-1 cells (*3*), we assayed nucleotidase activity using a variety of substrates and divalent cations and determined the effects of pH and ionic strength on enzymatic activity. The ADPase and GDPase activities were measured at 2.5 mM total nucleotide concentrations in the absence of divalent cations, as well as in the presence of either 0.5 or 5 mM $CaCl_2$, $MgCl_2$, $MnCl_2$, $SrCl_2$, $CuCl_2$, $CoCl_2$, or $NiCl_2$. Nucleotidase activity was only detected in the presence of calcium ions. Next, a variety of nucleoside mono-, di-, and triphosphates were used as substrates (2.5 mM final nucleotide concentrations) in the presence of 10 mM $CaCl_2$ (Figure 3). The activity for preferred substrates, GDP, IDP, and UDP, is high, in the range of 30000 (μmol of P_i/mg)/h, whereas the specific activity for ADP, CDP, and the nucleoside triphosphates is 20−50-fold lower. No measurable hydrolysis of either AMP or GMP was detected in parallel experiments (data not shown).

The effect of pH on the ADPase activity of hSCAN-1 was measured in 50 mM PIPES (pK_a 6.8) and 50 mM Bis-Tris (pK_a 6.5) buffers. Figure 4A shows that the pH optimum is in the range of 6.3−6.7. These values are slightly different from the pH optimum of approximately 6.8 obtained in a Bis-Tris buffer system for hSCAN-1 expressed in mammalian COS cells (*3*). Interestingly, there is a significant difference in enzyme activity at any given pH in the different buffer systems used. It should be noted that the substrate concentration used in these experiments was 2.5 mM ADP or GDP. Due to the relatively large K_m for ADP (5.4 ± 0.3 mM), versus the K_m for GDP (0.46 ± 0.09 mM), the substrate concentration of 2.5 mM was not optimal for the hydrolysis of ADP. However, our purpose was to compare nucleotide hydrolysis under the same conditions, including substrate concentrations, with pH as the only variable.

The effect of ionic strength on hSCAN-1 enzymatic activities (using a 2.5 mM concentration of each nucleotide) is shown in Figure 4B. NaCl inhibited hydrolysis of ADP more than hydrolysis of GDP. At 200 mM NaCl, ADPase and GDPase activities were reduced by about 70% and 30%, respectively, as compared with nucleotidase activities in the absence of NaCl.

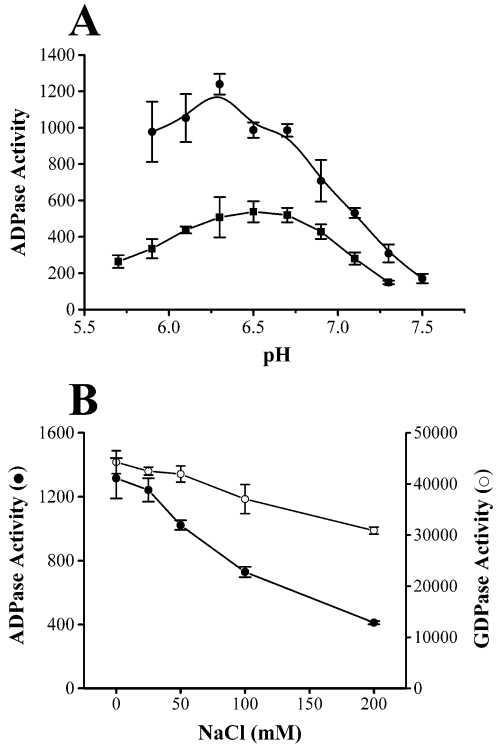

FIGURE 4: Biochemical characterization of hSCAN-1. In all cases, the nucleotide concentration used was 2.5 mM. (A**)** Effect of pH and type of buffer on the ADPase activity of hSCAN-1. Two different buffers having pK_a values from 6.5 to 7.0 were compared: (●) 50 mM PIPES (pK_a 6.8), 5 mM $CaCl_2$; (■) 50 mM Bis-Tris (pK_a 6.5), 5 mM $CaCl_2$. The error bars represent the standard deviation of the mean ($n = 3$). **(**B**)** Effect of ionic strength on the ADPase and GDPase activity of hSCAN-1. Varying amounts of NaCl were added to 20 mM MOPS, 5 mM $CaCl_2$, pH 7.1, and nucleotidase activity was measured as described in the Materials and Methods. The error bars represent the standard deviation of the mean ($n = 3$). Activity units in (A) and (B) are micromoles of P_i liberated per milligram of protein per hour at 37 °C.

The K_m for hydrolysis of a preferred nucleotide (GDP) and a nonpreferred nucleotide (ADP) were determined under conditions resulting in less than 10% of the added nucleotides hydrolyzed during the course of the experiments, thus allowing the use of the standard, simplified kinetic equations to fit the data obtained. The data were fit to hyperbolic curves to calculate the K_m and V_{max} for the purified enzyme for these nucleotides. The concentrations of metal−nucleotide complexes Ca−GDP and Ca−ADP and K_m for these substrate complexes were also calculated. For GDP hydrolysis in the presence of 5 mM $CaCl_2$, values of $K_m = 0.46 \pm 0.09$ mM (for GDP), $K_m = 0.39 \pm 0.08$ mM (for Ca−GDP), and $V_{max} = 45800 \pm 2100$ (μmol/mg)/h were obtained (the mean values ± standard deviations of four experiments). Likewise, for ADP hydrolysis in the presence of 10 mM $CaCl_2$, values of $K_m = 5.4 \pm 0.3$ mM (for ADP), $K_m = 4.7 \pm 0.3$ mM (for Ca−ADP), and $V_{max} = 4170 \pm 40$ (μmol/mg)/h were obtained (the mean values ± standard deviations of four independent experiments). Thus, the preferred substrate GDP has a lower K_m, but the K_m values for both GDP and ADP are fairly high, as compared to K_m values for the eNTPDase family of apyrases. All of the eNTPDases have K_m values less than 0.5 mM; the naturally soluble forms have higher K_m values (e.g., a K_m for GDP for NTPDase6 (CD39L2) of 211 μM (*18*)) than the membrane-bound, tetrameric forms, which have K_m values for ADP and ATP in the range of 10−100 μM (*19*).

Thus, the properties of the bacterially expressed and refolded hSCAN-1 mimic what is known of the properties of the mammalian cell expressed hSCAN-1 and differentiate it from other classes of soluble nucleotidases, including the eNTPDases (*1*, *20*).

Ca^{2+} Dependence of hSCAN-1 Activity. The GDPase activity of hSCAN-1 was absolutely dependent on the presence of Ca^{2+} (Figure 5, filled symbols). Surprisingly, GDPase activity did not increase in a quasi-linear fashion at total Ca^{2+} concentrations below 1 mM as would be expected if Ca^{2+} were only used as a cosubstrate for the nucleotide substrate. This "lag phase" at total Ca^{2+} concentrations below 1 mM and the overall sigmoidal shape of the activity curves can be seen in Figure 5A. For comparison, the GDPase activity of potato apyrase (a member of the eNTPDase family) was also determined at various Ca^{2+} concentrations (Figure 5, open symbols). Potato apyrase demonstrated a typical quasi-linear increase of enzymatic activity at the lowest Ca^{2+} concentrations used, as expected if Ca^{2+} functioned solely to form a Ca−GDP substrate complex suitable for enzymatic hydrolysis (Figure 5). Due to the chelating properties of GDP, free Ca^{2+} concentrations differ from total Ca^{2+} concentrations, especially at the lowest total Ca^{2+} concentrations used. Accordingly, replotting GDPase activity versus calculated free Ca^{2+} concentration also showed the lag phase in hSCAN-1 enzymatic activity at free Ca^{2+} concentrations below 0.1 mM (Figure 5B). No hSCAN-1 activity was detected at or below 60 μM free Ca^{2+} (Figure 5B, inset). In contrast, the GDPase activity of potato apyrase increased in a quasi-linear fashion at the lowest free Ca^{2+} concentrations used. Replotting GDPase activity versus calculated Ca−GDP complex concentration also demonstrated a lag phase for hSCAN-1 with no detectable activity below 0.25 mM Ca−GDP (Figure 5C). hSCAN-1 activity became detectable when the free Ca^{2+} concentration was increased to 87 μM (Figure 5B, filled circles), which occurred at about 0.3 mM Ca−GDP (Figure 5C). In contrast, the GDPase activity of potato apyrase increased in a typical quasi-linear manner at Ca−GDP concentrations below 0.25 mM (Figure 5C).

The presence of 100 mM NaCl accentuated the lag phase of the hSCAN-1 activity curve, with no enzymatic activity detectable at or below 126 μM free Ca^{2+} (Figure 5B, inset, filled squares). In the presence of NaCl, the activity curve was slightly shifted to higher Ca−GDP concentrations (Figure 5C). Figure 5C also shows that the enzymatic activation of hSCAN-1 in the presence of NaCl occurred at a much higher free Ca^{2+} concentration (200−300 μM), as compared to approximately 100 μM free Ca^{2+} in the absence of NaCl (the free Ca^{2+} concentrations are indicated by arrows and numbers in Figure 5C).

Qualitatively similar results demonstrating the lack of hSCAN-1 activity at or below 60 μM free Ca^{2+} were also obtained using ADP as substrate (data not shown). The nonlinear dependence of nucleotidase activity on submillimolar total Ca^{2+} concentrations and virtual inactivity of the enzyme below 60 μM free Ca^{2+} (in the absence of NaCl) or 120 μM free Ca^{2+} (in the presence of NaCl) suggested that Ca^{2+}-induced conformational changes might occur in hSCAN-1 in this range of Ca^{2+} concentrations.

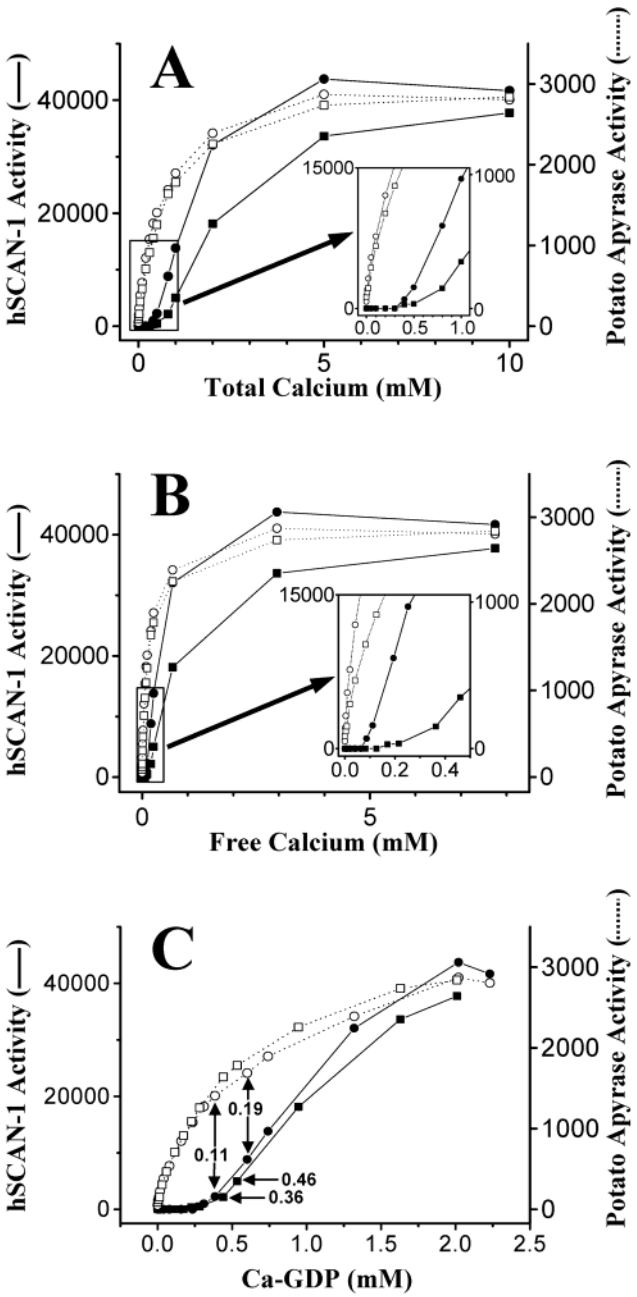

FIGURE 5: Ca^{2+} dependence of hSCAN-1 and potato apyrase GDPase activities. GDPase activities of hSCAN-1 (solid lines, filled symbols) and potato apyrase (dotted lines, open symbols) were measured in 20 mM MOPS, pH 7.1, in either the absence (●, ○) or the presence (■, □) of 100 mM NaCl. The total GDP concentration was 2.5 mM, and total Ca^{2+} concentrations were varied as indicated in the top panel (A). (A) hSCAN-1 and potato apyrase GDPase activities as a function of total Ca^{2+} concentration. The inset expands a portion of the graph corresponding to low total Ca^{2+} concentrations. (B) hSCAN-1 and potato apyrase GDPase activities as a function of free Ca^{2+} concentration, replotting the data presented in panel (A) versus free Ca^{2+} concentration. Free Ca^{2+} concentrations were calculated as described in the Materials and Methods. The inset expands a portion of the graph corresponding to low free Ca^{2+} concentrations. (C) hSCAN-1 and potato apyrase GDPase activities as a function of Ca−GDP concentration, replotting the data presented in panel (A) versus Ca−GDP concentration. Ca−GDP concentrations were calculated as described in the Materials and Methods. The numbers in panel (C) denote calculated free Ca^{2+} concentrations for the indicated data points. Note that the enzymatic activity of hSCAN-1 in the presence of NaCl occurs at higher free Ca^{2+} concentrations (200−300 μM) than in the absence of NaCl (approximately 100 μM). Activity units are micromoles of P_i liberated per milligram of protein per hour at 37 °C.

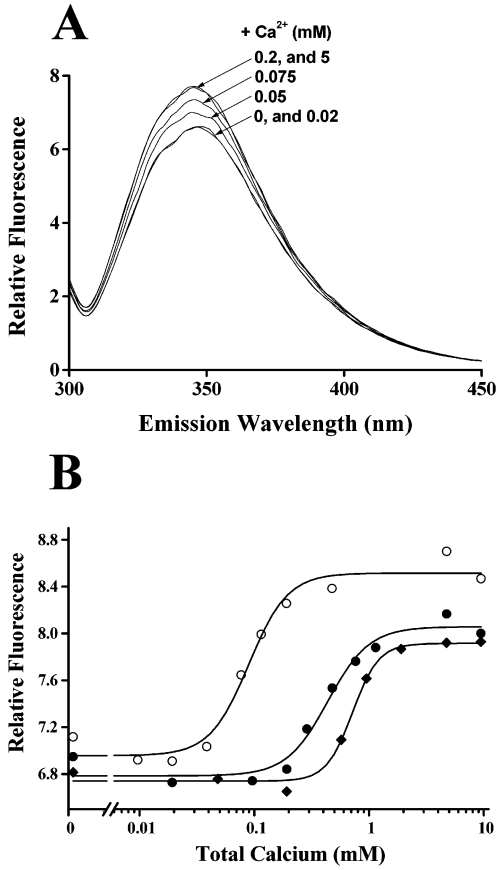

FIGURE 6: Effect of Ca^{2+} on the intrinsic tryptophan fluorescence of hSCAN-1. (A) Change in the intrinsic tryptophan fluorescence as a function of added Ca^{2+}. A 0.85 μM (32 μg/mL) concentration of hSCAN-1 in 20 mM MOPS, pH 7.1, was excited at 295 nm, and fluorescence emission was recorded before and after stepwise additions of $CaCl_2$ to the final concentrations indicated. Note that the fluorescence intensity increases in a saturable manner upon addition of Ca^{2+} with half-saturation at about 70 μM Ca^{2+}. (B) Saturable increase in hSCAN-1 tryptophan fluorescence caused by Ca^{2+}, and the effects of NaCl and Mg^{2+}. Emission spectra were obtained in 20 mM MOPS, pH 7.1 (○), in 20 mM MOPS, pH 7.1, containing 100 mM NaCl (●), and in 20 mM MOPS, pH 7.1, containing 5 mM $MgCl_2$ (◆). The excitation was at 295 nm, and the spectra were taken before and after stepwise addition of $CaCl_2$. Fluorescence intensities at λ_{max} (346−348 nm) were corrected for dilution and plotted against final concentrations of added Ca^{2+}. The lines represent plots of the four-parameter logistic fits to the data, from which the EC_{50} values are obtained.

Ca^{2+}-Induced Conformational Changes in hSCAN-1. We investigated the conformational changes in hSCAN-1 by analyzing the intrinsic tryptophan fluorescence of the purified enzyme as a function of Ca^{2+} concentration. Figure 6A shows the emission spectra from excitation at 295 nm of 11 tryptophan residues present in the protein. Stepwise addition of Ca^{2+} caused a saturable increase in the intensity of tryptophan fluorescence with half-saturation at about 70 μM Ca^{2+}. No shift in the maximum fluorescence wavelength (346−348 nm) was detected. The Ca^{2+}-induced increase of tryptophan emission was completely reversible upon addition of EDTA (0.2 mM $CaCl_2$ followed by addition of 0.5 mM EDTA, data not shown). In the absence of Ca^{2+}, $MgCl_2$ at 5 mM did not affect tryptophan fluorescence, indicating cation selectivity of the conformational change (data not shown). Concentrations of Ca^{2+} required to generate 50% of the maximal change in tryptophan emission increased from 88 ± 22 μM (mean ± SD, $n = 5$) in 20 mM MOPS to about

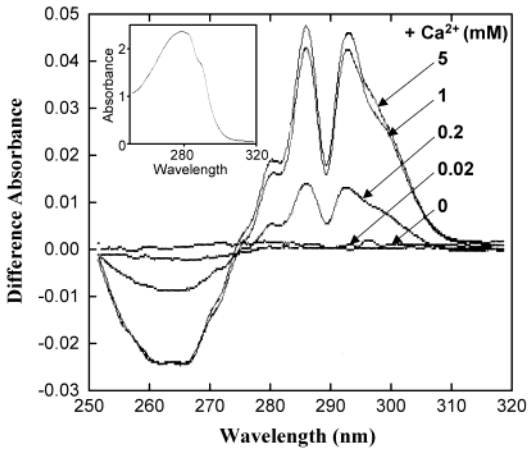

FIGURE 7: Ca^{2+}-induced difference absorption spectra of hSCAN-1. Both sample and reference cells contained 0.5 mL of 25 μM hSCAN-1 (0.96 mg/mL) in 20 mM MOPS, pH 7.1, 100 mM NaCl. The difference spectra were recorded starting with no added Ca^{2+}, and after stepwise addition of $CaCl_2$ to the sample cell in 2 μL aliquots to the final Ca^{2+} concentrations indicated. To adjust the protein concentration, the same volumes of water were added to the reference cell. Note that the magnitude of the differential absorbance increases in a saturable manner upon addition of Ca^{2+} and reaches half-saturation at a Ca^{2+} concentration between 0.2 and 1 mM. The inset shows th absorption spectrum of hSCAN-1 in the absence of Ca^{2+}.

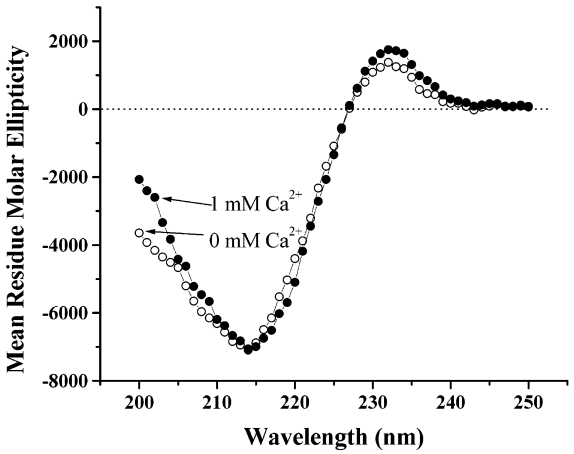

FIGURE 8: CD spectra of hSCAN-1 protein in the absence and presence of 1 mM Ca^{2+}. The pure hSCAN-1 protein was analyzed at a concentration of 4.24 μM (0.16 mg/mL) in 10 mM Tris−HCl buffer, pH 7.1, in the absence (open circles) and presence (filled circles) of 1 mM Ca^{2+}. Values plotted are the mean residue molar ellipticity in (deg·cm^2)/(dmol·residue).

400 μM in the presence of 100 mM NaCl and approximately 700 μM in the presence of 5 mM $MgCl_2$ (Figure 6B). Remarkably, NaCl affected the Ca^{2+} dependence of tryptophan fluorescence in a similar manner as it shifted the lag phase of the nucleotidase activity curve to higher Ca^{2+} concentrations (Figure 5B). This suggests a causal relationship between the conformational change detected by tryptophan fluorescence and the enzymatic activation of hSCAN-1 detected by nucleotidase assay.

We further analyzed Ca^{2+}-dependent conformational changes in hSCAN-1 by UV spectroscopy (Figure 7). These experiments were conducted in the presence of 100 mM NaCl in 20 mM MOPS, pH 7.1. The UV spectrum of hSCAN-1 is typical for a protein rich in Tyr (14 residues) and Trp (11 residues) with a characteristic shoulder at 290−295 nm due to tryptophan residues (see the inset in Figure 7). Addition of 2 mM Ca^{2+} caused a distinct red shift of the whole spectrum of about 0.5 nm, as well as a slight increase in the maximum absorbance (from 2.354 to 2.370 for a protein solution of 0.96 mg/mL concentration) and a small shift of λ_{max} from 278.9 to 279.1 nm (data not shown). Addition of 5 mM Mg^{2+} to hSCAN-1 did not influence the UV spectrum, but subsequent addition of 2 mM Ca^{2+} did result in a red shift and an increase in the maximum of the spectrum (data not shown). The red shift of the UV spectrum suggests Ca^{2+}-induced rearrangements of Tyr and Trp residues, decreasing their exposure to the aqueous solvent.

The difference UV spectra demonstrated Ca^{2+}-dependent, saturable changes in the absorbance of Trp residues (peak at 293 nm) and Tyr residues (peak at 286 nm). The smaller peak at 280 nm is likely a second maximum for Tyr residues. The contribution of Phe residues to the difference spectra in the range of 250−270 nm is very small. The changes in the UV absorption of Tyr and Trp residues reached half-maximum values at a Ca^{2+} concentration between 0.2 and 1 mM and were specific for Ca^{2+}, since addition of 5 mM Mg^{2+} did not result in a measurable difference spectrum (data not shown). Since these experiments were performed in the presence of 100 mM NaCl in 20 mM MOPS, pH 7.1 (the NaCl stabilizes the protein and prevents aggregation at higher protein concentrations), the half-saturating Ca^{2+} concentration in the range of 0.5 mM corresponds well to a Ca^{2+} concentration required for tryptophan fluorescence change under the same buffer and ionic strength conditions (see Figure 6B). The Ca^{2+}-induced increase in both tyrosine and tryptophan absorbance suggests rearrangements to a less polar environment, with the magnitude of the effect indicating that multiple tyrosine and tryptophan residues are involved, suggesting a delocalized conformational change in the protein.

Circular Dichroism Spectroscopy of hSCAN-1. To further characterize the hSCAN-1 protein and the conformational change induced by Ca^{2+}, CD spectra were obtained in the presence and absence of 1 mM Ca^{2+}. The CD spectra were obtained in 10 mM Tris−HCl, pH 7.1, rather than 20 mM MOPS, pH 7.1, used for the fluorescence and UV absorption studies, due to the high absorbance of 20 mM MOPS buffer below 240 nm. Repeating the tryptophan fluorescence experiments in 10 mM Tris−HCl, pH 7.1, buffer gave a EC_{50} value for Ca^{2+} similar to that obtained in 20 mM MOPS, pH 7.1, buffer (not shown). The CD spectra shown (Figure 8) are representative of three experiments performed in the presence and absence of 1.0 mM $CaCl_2$. Upon addition of 1 mM $CaCl_2$, there are minor increases in the amplitude of the positive peak at about 232 nm and the position of the negative peak at about 214 nm in the CD spectra, as well as small changes below 205 nm (see Figure 8). The PROF computer program (*17*) predicted the amounts of secondary structures based on the 339 amino acid sequence of hSCAN-1 to be 11.5% α-helix, 44.5% β-sheet, and 44% random coil. Analysis of the experimentally obtained CD data by the neural network K2D computer program (*16*) in the absence of Ca^{2+} calculated the amounts of secondary structures present in hSCAN-1 as being 9.7 ± 1.2% α-helix, 44 ± 2.3% β-sheet, and 46.3 ± 0.6% random coil, consistent with the PROF-predicted secondary structure composition. The pres-

ence of 1 mM Ca^{2+} caused no statistically significant change in the secondary structure of hSCAN-1, with the K2D program calculating 10.3 ± 1.2% α-helix, 43 ± 3% β-sheet, and 46.7 ± 0.6% random coil in the presence of 1 mM Ca^{2+}.

Evaluation of the Possibility of Ni^{2+}Ion Contamination Effects on hSCAN-1 Properties. We performed additional experiments to investigate whether the "lag" in Ca^{2+}-induced activation of hSCAN-1 could be due to potential Ni^{2+} contamination arising from the Ni−NTA column that was used to purify the enzyme. An hSCAN-1 inclusion body preparation was solubilized in guanidine−HCl, applied to the Ni−NTA resin under denaturing conditions, eluted, and treated with Chelex-100 resin (while still denatured in 6 M guanidine−HCl) to remove all contaminating divalent cations. The Chelex-treated hSCAN-1 preparation was purified as described above, and the calcium activating studies were repeated. We observed no differences in either the Ca^{2+} dependence of GDPase activity or the Ca^{2+}-induced conformational change as monitored by tryptophan fluorescence (data not shown), indicating that potential Ni^{2+} contamination is not responsible for these unique properties of hSCAN-1.

DISCUSSION

The high specific activity of the bacterially expressed, refolded, and purified hSCAN-1 apyrase (28000−44000 (μmol/mg)/h for the hydrolysis of GDP) compares favorably to that of both the naturally folded enzyme synthesized in the in vitro bacterial rapid translation system (28000 (μmol/mg)/h) and the COS cell expressed enzyme described recently (*3*). This, along with the absence of any evidence of conformational heterogeneity detected by size exclusion chromatography (Figure 2) and native gel electrophoresis (Figure 1B), strongly suggests that the large majority of the protein molecules are refolded into a native, enzymatically active conformation.

hSCAN-1 was discovered (*3*) by sequence homology with the blood-sucking insect apyrases (*2*) and shares 45% amino acid sequence identity with the *Cimex* bed bug apyrase (*2*, *3*). The enzymatic activity of both enzymes is strictly dependent on Ca^{2+}. However, the substrate profiles of hSCAN-1 and the bed bug apyrase differ. The bed bug apyrase hydrolyzes ADP and ATP efficiently, whereas hSCAN-1 hydrolyzes UDP, GDP, and IDP 20−50-fold faster than ADP and CDP and hydrolyzes ATP only to a very small extent (see Figure 3). The ADPase specific activity reported for the *Cimex* bed bug apyrase is 379 units/mg (*2*), equivalent to 22740 (μmol/mg)/h. This ADPase specific activity is comparable to the GDPase specific activity of hSCAN-1 reported in this work (28000−44000 (μmol/mg)/h).

Bacterially expressed hSCAN-1 has a nucleotidase profile (Figure 3) similar to that of the enzyme expressed in mammalian COS cells (*3*). Thus, the specific activity of hSCAN-1 expressed in COS cells for GDP and UDP is approximately 100-fold greater than that for ADP. It was previously reported that the COS cell expressed hSCAN-1 displayed nucleotidase activity with calcium, but not magnesium, ions (*3*). This was also found to be the case for the bacterially expressed enzyme described in this work. In addition, the bacterially expressed and refolded enzyme was not activated by any other divalent cations tested, including manganese, strontium, copper, cobalt, and nickel, indicating that it is indeed specific for calcium ions, unlike the eNTPDase apyrases.

The pH optimum of bacterially expressed hSCAN-1 is 6.3−6.7 (Figure 4A) and is comparable to the pH profile of COS expressed hSCAN-1, but lower than the optimum pH of 8.5 for the bed bug apyrase (*2*, *3*). Unlike the *Cimex* bed bug apyrase, both the bacterially expressed and COS cell expressed hSCAN-1 show a relatively sharp decline of activity above pH 7.0.

The hSCAN-1 K_m values for ADP (5.4 mM) and GDP (0.46 mM) are high and, especially for ADP, are substantially higher than the 10−100 μM range of K_m values reported for the membrane-bound eNTPDase apyrases (*19*), as well as the 211 μM GDP K_m reported for the soluble NTPDase6 apyrase (CD39L2; *18*). Thus, the soluble apyrase described in this work should only be fully enzymatically active in microenvironments having high concentrations of nucleotides, as are the soluble eNTPDases.

The most unique and surprising feature of hSCAN-1 is the absolute need for Ca^{2+} for enzymatic activity. Unexpected nonlinear dependence of nucleotidase activity on submillimolar Ca^{2+} concentrations and virtual inactivity of the enzyme below 60 μM free Ca^{2+} (in the absence of NaCl) or 120 μM free Ca^{2+} (in the presence of NaCl) prompted us to investigate the possibility of structural changes in the protein as a function of Ca^{2+} concentration. The intrinsic fluorescence and difference absorption studies of hSCAN-1 revealed substantial Ca^{2+}-induced changes in the environment of tryptophan and tyrosine residues. Several aspects of these conformational changes are of particular interest.

First, conformational changes occur in a saturable manner with respect to Ca^{2+} concentrations, suggesting that hSCAN-1 is a calcium-binding protein. The estimated affinity of hSCAN-1 for Ca^{2+} obtained from the Ca^{2+} concentration required to induce a half-maximal conformational change (EC_{50}) was approximately 88 μM. This apparent affinity for Ca^{2+} is in the range of the dissociation constants for Ca^{2+} in specialized Ca^{2+}-binding proteins such as EF-hand type S100 proteins (*21*, *22*).

Second, the magnitude of Ca^{2+}-induced changes in the Tyr and Trp environment, as evident from the red shift of the UV absorption spectra and the size and shape of the UV difference spectra, suggests a nonlocalized "global" change in protein conformation. The Ca^{2+}-induced UV difference spectrum shown in Figure 7 has the same shape, but opposite sign, as compared to difference spectra obtained with proteins rich with Tyr and Trp after their denaturation with Gu−HCl. Thus, the difference absorbance spectrum of hSCAN-1 between 275 and 305 nm increases with added Ca^{2+} in Figure 7, whereas the absorbance in this wavelength region decreases during the process of protein denaturation (*23*, *24*). This suggests that, upon addition of Ca^{2+}, several aromatic residues become less exposed to the aqueous solvent, probably as a result of shifting into a more hydrophobic environment. Interestingly, this conformational change is not accompanied by major changes in secondary structure (see Figure 8), suggesting a reshaping of the tertiary structure of the enzyme with little change in secondary structural elements.

Third, there is a qualitative correlation between free Ca^{2+} concentrations required for conformational changes in hSCAN-1 and free Ca^{2+} concentrations needed for enzymatic

activation of the protein. Thus, the GDPase activity of hSCAN-1 became detectable at free Ca^{2+} concentrations of about 90 and 300 μM when assayed in either the absence or the presence of 100 mM NaCl, respectively (Figure 5B, inset). Comparably, the changes in tryptophan fluorescence become noticeable at similar free Ca^{2+} concentrations (Figure 6B). However, the EC_{50} of free Ca^{2+} for the conformational change does not correlate quantitatively with that for the nucleotidase activity. Given $EC_{50} = 0.088$ mM free Ca^{2+} for the conformational change and $K_m = 0.39$ mM for Ca−GDP, one would expect nucleotidase activity of 1/2 of $V_{max}/2$ (i.e., $V_{max}/4$) at a substrate concentration equal to K_m and a free Ca^{2+} concentration equal to 0.088 mM. In fact, the nucleotidase activity of hSCAN-1 is much lower than 11000 ($V_{max}/4$) at 0.39 mM Ca−GDP and 0.11 mM free Ca^{2+} (Figure 5C), suggesting that some other factor(s) may decrease the affinity of the enzyme for Ca^{2+} or that some other processes affecting enzyme activity may be involved. In view of the strong effects of ionic strength and divalent Mg^{2+} ions on the EC_{50} for conformational change (Figure 6B), it is possible that the presence of 2.5 mM GDP in the nucleotidase assay solutions may also decrease the affinity of the enzyme for Ca^{2+}. Due to the high absorbance of nucleotides at millimolar concentrations, the Ca^{2+} titration of tryptophan fluorescence in the presence of nucleotide was not performed. While some additional, not yet identified, factors may affect the nucleotidase activity of hSCAN-1, the results suggest a causal relationship between the Ca^{2+}-induced conformational change in hSCAN-1 and the enzymatic activation of the protein.

The physiological relevance of Ca^{2+}-dependent activation of hSCAN-1 is largely speculative due to scarce information about the localization and function of this enzyme in vivo, since this soluble human apyrase was discovered only very recently (*3*). The localization of hSCAN-1 may be very important for efficient inactivation of the enzyme in intracellular compartments with low Ca^{2+} concentrations or elevated pH, where nucleotidase activity could be detrimental to the cell. The mRNA distribution of hSCAN-1 showed the highest levels of hSCAN-1 in testes, prostate, placenta, and small intestine, with lower levels present in lung, stomach, salivary gland, colon, spleen, and thymus tissues (*3*). hSCAN-1 was not detectable in human sera by Western blot using a specific anti-hSCAN-1 antibody (T. Smith, personal communication).

In summary, this is the first study demonstrating that a human apyrase can be bacterially expressed and efficiently refolded into an active nucleotidase, which is fully enzymatically functional and virtually indistinguishable from the mammalian cell expressed apyrase. This indicates that posttranslational modifications that cannot be performed by bacteria, including glycosylation, are not necessary for the proper folding and enzymatic activity of hSCAN-1 apyrase. This is also the first demonstration that an apyrase is a calcium-binding protein and that a Ca^{2+}-induced conformational change may be required for activation of the enzyme. Future studies may provide more details as to the number and structure of the hSCAN-1 Ca^{2+}-binding sites, the unusual nature of the Ca^{2+}-induced conformational change, and the physiological relevance of Ca^{2+} activation of hSCAN-1.

ACKNOWLEDGMENT

We thank Drs. James Ball and Stefan Paula for use of the fluorescence instrument and for help with the fluorescence measurements, Dr. A. M. Stalcup for use of the circular dichroism instrument and for help with the circular dichroism measurements, and Dr. Thomas Smith for discussions concerning the properties of the mammalian cell expressed hSCAN-1.

REFERENCES

1. Zimmermann, H., Beaudoin, A. R., Bollen, M., Goding, J. W., Guidotti, G., Kirley, T. L., Robson, S. C., and Sano, K. (1999) in *Second International Workshop on Ecto-ATPases and Related Ectonucleotidases* (Vanduffel, L., Ed.) pp 1−9, Shaker Publishing BV, Maastricht, The Netherlands, Diepenbeek, Belgium.
2. Valenzuela, J. G., Charlab, R., Galperin, M. Y., and Ribeiro, J. M. (1998) *J. Biol. Chem. 273*, 30583−90.
3. Smith, T. M., Hicks-Berger, C. A., Kim, S., and Kirley, T. L. (2002) *Arch. Biochem. Biophys. 406*, 105−115.
4. Gayle, R. B., Maliszewski, C. R., Gimpel, S. D., Schoenborn, M. A., Caspary, R. G., Richards, C., Brasel, K., Price, V., Drosopoulos, J. H. F., Islam, N., Alyonycheva, T. N., Broekman, M. J., and Marcus, A. J. (1998) *J. Clin. Invest. 101*, 1851−9.
5. Mihaylova-Todorova, S., Todorov, L. D., and Westfall, D. P. (2001) *J. Pharmacol. Exp. Ther. 296*, 64−70.
6. Burnstock, G. (1996) *Lancet 347*, 1604−1605.
7. Chizh, B. A., and Illes, P. (2001) *Pharmacol Rev. 53*, 553−68.
8. Stoscheck, C. M. (1990) *Anal. Biochem. 184*, 111−116.
9. Laemmli, U. K. (1970) *Nature (London) 227*, 680−685.
10. Fiske, C. H., and Subbarow, Y. (1925) *J. Biol. Chem. 66*, 375−400.
11. Treuheit, M. J., Vaghy, P. L., and Kirley, T. L. (1992) *J. Biol. Chem. 267*, 11777−11782.
12. Smith, T. M., and Kirley, T. L. (1999) *Biochemistry 38*, 321−328.
13. Bers, D., Patton, C., and Nuccitelli, R. (1994) A Practical Guide to the Study of Ca^{2+} in Living Cells, *Methods in Cell Biology*, Vol. 40, pp 3−29, Academic Press, San Diego.
14. Martell, A., and Smith, R. (1975) *Critical Stability Constants*, Vol. 2, Plenum Publishing Corp., New York.
15. Geourjon, C., and Deleage, G. (1993) *Comput. Appl. Biosci. 9*, 87−91.
16. Andrade, M. A., Chacon, P., Merelo, J. J., and Moran, F. (1993) *Protein Eng. 6*, 383−90.
17. Ouali, M., and King, R. D. (2000) *Protein Sci. 9*, 1162−76.
18. Braun, N., Fengler, S., Ebeling, C., Servos, J., and Zimmermann, H. (2000) *Biochem. J. 351*, 639−647.
19. Zimmermann, H. (1999) *Trends Pharmacol. Sci. 20*, 231−6.
20. Plesner, L. (1995) *Int. Rev. Cytol. 158*, 141−214.
21. Schafer, B. W., and Heizmann, C. W. (1996) *Trends Biochem. Sci. 21*, 134−40.
22. Donato, R. (2001) *Int. J. Biochem. Cell Biol. 33*, 637−68.
23. Schmid, F. X. (1997) in *Protein Structure: A Practical Approach* (Creighton, T. E., Ed.) pp 261−297, Oxford University Press, Oxford.
24. Schwaller, B., Durussel, I., Jermann, D., Herrmann, B., and Cox, J. A. (1997) *J. Biol. Chem. 272*, 29663−71.

BI026763B